Limnol. Oceanogr., 48(6), 2003, 2303–2313

Bioaccumulation of silver-110m, cobalt-60, cesium-137, and manganese-54 by the freshwater algae *Scenedesmus obliquus* and *Cyclotella meneghiana* and by suspended matter collected during a summer bloom event

Christelle Adam and Jacqueline Garnier-Laplace
Centre d'Etudes de Cadarache, Institut de Radioprotection et de Sûreté Nucléaire, Laboratoire de Radioécologie Expérimentale. Bâtiment 186, B.P. 3-13115 Saint-Paul-lez-Durance Cedex, France

Abstract

Laboratory experiments were done to assess ^{110m}Ag, ^{60}Co, ^{137}Cs, and ^{54}Mn uptake by two phytoplankton species, the chlorophyte *Scenedesmus obliquus* and the small diatom *Cyclotella meneghiana.* Mn and Co were characterized by similar uptake kinetic rates, 20–30 d^{-1}, whatever the algal species, whereas depuration rates were 3–60 d^{-1}. Silver uptake and depuration rates were very high (144–293 d^{-1}). However, Cs accumulation and depuration were very slow, with kinetic constants of 0.6–5 d^{-1}. Mn, Co, and Ag were more strongly accumulated by *C. meneghiana* than *S. obliquus* and vice versa for Cs. To evaluate the extrapolation of the kinetic rates fitted for *S. obliquus* and *C. meneghiana* to natural conditions, suspended solids were also collected during a bloom event and contaminated. Radionuclide exchange between three distinct compartments among the suspended solids was modeled: the kinetic rates fitted for *S. obliquus* and *C. meneghiana* were used to represent chlorophyte and bacillariophyte contamination, whereas kinetic rates describing a third compartment were estimated when possible. A third compartment was evidenced only for Mn and Co, whereas, for Ag, the chlorophyte and bacillariophyte compartments were sufficient to describe the particulate phase. For Cs, algae kinetic rates could not be used, so a single compartment was fitted. These experiments confirm the low affinity of Cs for phytoplankton and the high bioavailability of Ag. In the case of Co and Mn, several processes acting simultaneously govern the contamination of natural suspended solids.

Waterways constitute an important group of natural resources, habitats, and living organisms that need protection from various stress factors, including radionuclide releases. Freshwaters can receive low-level radioactive liquid wastes discharged from nuclear facilities under normal operating conditions or may be accidentally contaminated such as occurred during the Chernobyl accident.

Algae play a key role in the radioactive contamination of freshwater ecosystems, as a point of entry of pollutants within trophic nets and because they can accumulate radionuclides very quickly to a high level. Algal blooms in eutrophic rivers may lead to high biomasses whose impact on the contamination of higher trophic levels in freshwater bodies, as well as on the radionuclide fluxes from the water column to the sediment compartment by sedimentation or from the continent to the sea, must be considered. The behavior of manganese during phytoplankton blooms has been extensively studied using ^{54}Mn to assess the importance of oxidation processes in its biogeochemical cycle (Sunda and Huntsman 1987; Kudo et al. 1992; Moffett 1994; Schoemann et al. 1998). The biological control of other radionuclides partitioning between liquid and solid phases has been very poorly studied. Moreover, most of the studies were undertaken in nutritive media whose chemical composition was completely different from that of natural waters and with green algae, which are not always representative of natural phytoplankton populations. Diatoms, for instance, may represent >90% of the phytoplanktonic population during early summer in the French river Loire (Lair and Reyes-Marchant 1997). Despite this abundance, they have rarely been studied in the field of freshwater radioecology.

The present article focuses on the kinetics of radionuclide uptake by phytoplankton. The radionuclides investigated (^{60}Co, ^{54}Mn, ^{137}Cs, and ^{110m}Ag) are among the major radionuclides (except tritium) released by a nuclear power plant under normal operating conditions. They exhibit contrasting behaviors, depending on the biochemical properties of their stable isotopes. Cobalt and manganese are two essential elements for phytoplankton growth (Sunda 1988). Cesium is a chemical analogous to potassium that is classified among the macronutrients. Silver belongs to the ''very toxic'' elements (Florence et al. 1992).

The present results are part of a wider research program undertaken to analyze and model radionuclide transfers through a simplified trophic chain representative of the pelagic net of the Vienne River, a tributary of the Loire River (France), influenced by radioactive releases from the Civaux nuclear power plant. The experiment was divided into two consecutive phases. During the first phase, two algal species (*Cyclotella meneghiana* and *Scenedesmus obliquus*), which were selected as biological models representative of the Vienne River spring and summer algal blooms, respectively, were used to study the radionuclide uptake by phytoplankton. During a second phase, natural suspended matter was collected in situ during a summer bloom period and brought back to the laboratory to be contaminated with radionuclides. The knowledge of the contamination kinetics of diatoms and green algae acquired during the first experiments using *C. meneghiana and S. obliquus* was used to evaluate the importance of the algal component in the radioactive contamination of natural suspended solids.

Acknowledgments

We thank Jean-Pierre Baudin for stimulating discussions about the data and Arlette Cazaubon for advice for the field work. Françoise Siclet provided assistance with selection of field collection dates.

Materials and methods

Algal cultures—*S. obliquus* and *C. meneghiana* original cells were obtained from the Plant Physiological Institute of the University of Göttingen. Stock cultures were maintained in modified B3N medium (Nichols and Bold 1965) and in f/2 medium (Guillard and Ryther 1962) for *S. obliquus* and *C. meneghiana*, respectively. The green algae *Scenedesmus* were grown in 3-liter glass flasks at 20 ± 1°C under cool white fluorescent lights (45 μmol quanta m^{-2} s^{-1}) on a 16 : 8 light : dark cycle, whereas *Cyclotella* was maintained on a 12 : 12 light : dark cycle at 15 ±1 °C. Air was filtered through a 0.22-μm acetate filter to limit bacterial contamination, before being bubbled continuously into the algal cultures to ensure an adequate supply of CO_2. Cell suspensions were kept well mixed with a magnetic stirrer.

Uptake experiments with the unicellular algae—In contrast to a large number of studies, uptake experiments were not done in a nutritive medium but in natural water, to increase the representativeness of the results. Natural water (pH 8.1, 9.7 mg L^{-1} Ca, 2.8 mg L^{-1} Mg, 11.4 mg L^{-1} Na, 2.8 mg L^{-1} K, 5.9 mg L^{-1} NO_3, 16 mg L^{-1} Cl, 9.9 mg L^{-1} SO_4, 35 mg L^{-1} HCO_3, and 5.5 mg L^{-1} dissolved organic carbon) was collected in the Vienne River. Preliminary experiments showed that keeping the two algal species in this water for 5 d did not induce any perturbation to their multiplication rate or morphology. The acclimation was done in two steps: at first, during a 7-d culture phase, the levels of stable manganese and cobalt concentrations in the nutritive medium (in the chemical forms of $MnCl_2$, $CoCl_2$, and B_{12} vitamin) were adjusted to the concentrations observed in the Vienne River by adding 20 μg L^{-1} of Mn and stopping the input of stable Co. Subsequently, algae were harvested on a 0.45-μm cellulose acetate membrane under very gentle vacuum and washed several times with filtered Vienne River water, to remove nutritive medium. They were then resuspended into 1-liter glass flasks that contained 0.45 μm filtered Vienne water. After this acclimation phase of 24 h, they were again harvested and resuspended in filtered Vienne water at a final cell density of $\sim 10^7$ and 10^6 cells ml^{-1} for *S. obliquus* and *C. meneghiana*, respectively, to be contaminated with radionuclides. Throughout the uptake experiments, cell suspensions were kept under the same light and temperature conditions as during the culture phase, in acid-washed flasks on a magnetic stirrer. The physiological fitness of the two species was evaluated by microscopic observation of cells, which showed photosynthetically active cells and no cell breakage induced by the experimental conditions. The resulting algal suspension was contaminated to a level of 30 Bq ml^{-1} for each individual radionuclide. The radioactive solutions were obtained from the Amersham International Radiochemical Centre, and each radionuclide was added to a separate flask in the chemical forms of $^{60}CoCl_2$, $^{137}CsCl$, $^{54}MnCl_2$, and $^{110m}AgNO_3$, respectively. Because of the presence of carrier element in commercialized radionuclide solutions, this radioactive contamination came with the addition of a stable element. Thus, the concentrations of stable cobalt, cesium, manganese, and silver during experiments were 5 ng L^{-1}, 20 ng L^{-1}, 90 ng L^{-1} and 2 μg L^{-1}, respectively. Except for Ag, the added trace metal concentrations were much lower than those of natural water and no modification, such as homeostasis control, had to be taken into account.

Natural suspended matter collected during a bloom event—For the second series of experiments, natural suspended matter was collected from the Vienne River during a summer bloom event in July. First, the water was filtered through a net with a mesh size of 70 μm, to eliminate most zooplankton species liable to graze phytoplankton. The resulting water was then brought back to the laboratory under dark conditions in 40-liter plastic carboys and maintained at 4°C to limit chemical and biological changes. Twenty-four hours after the sampling procedure, the suspensions were homogenized, split into 15-liter batches, and spiked with 30 Bq ml^{-1} of each radionuclide. The radioactive solutions were identical to those used for the contamination of *S. obliquus* and *C. meneghiana*, and the specific activity in particular was the same. The water was maintained at 21 ± 0.5°C under cool white fluorescent lights on a 16 : 8 light : dark cycle. The tanks were covered, to reduce evaporation.

Sampling and analysis—To monitor the radionuclide concentration of the particulate phase (unicellular algae or natural suspended matter), water samples were taken at time periods of 5, 10, 15, and 30 min, 1, 2, 4, and 8 h, and 1, 2, and 3 d. For the experiments that used *C. meneghiana* and *S. obliquus*, two samples were collected: one aliquot was used to estimate the total radionuclide concentration of the water, and the other was filtered through a 0.45-μm acetate membrane, to evaluate the contamination of the dissolved phase. The radionuclide concentration of the algal cells was deduced from the difference between the two measurements, divided by the algal mass. The latter was determined from cell counts that were related to the wet and dry weight using linear relationships calibrated during preliminary experiments.

For the experiment that used natural suspended solids, the particles were isolated from the water by filtration of a 200-ml suspension through a 0.45-μm cellulose acetate membrane. This technique had to be used because of the low particle density, to achieve greater accuracy on radioactivity as well as on mass measurements. Radionuclide retention on the 0.45-μm acetate membrane was checked by superimposing two filters, the second of which was representative of the blank. This ''blank'' activity was then subtracted from the measurements of the filter radioactivity to estimate the contamination of the suspended matter. This blank value was equal to 17% of the total activity in the case of ^{110m}Ag, whereas, for the other radionuclides, it was not significant. The filter was weighed before and after the filtration step, to determine the wet weight (ww) of suspended matter. The composition of particulate phase was analyzed by microscopic examination, and algal species were enumerated.

The radioactivity was measured by high-resolution gamma spectrometry using a high-purity germanium detector, in low background shield, coupled to a multichannel analyzer. The radionuclide activity in each sample was related to the

first day of the experiment, for correction of physical decay, and background counts were subtracted.

During the experiments, wall adsorption was monitored by checking the sum of the radionuclide concentration in dissolved and particulate phases. For the first experiments, using unicellular algae, total concentrations were recovered at >95% for the four radionuclides. For the experiments that used natural suspended solids, wall adsorption had to be taken into account for ^{137}Cs, because it represented ~36% of the total activity. For the three other radionuclides, it did not statistically differ from the measurement error.

Kinetic approach and assessment of equilibrium—For the unicellular algae contamination experiments, radionuclide uptake characteristics were determined using a kinetic model in which sorption processes were assumed to follow a simple first-order reversible reaction (Jannasch et al. 1988). R_{water} represents the sum of all dissolved forms of radionuclide and R_{algae} the radionuclide associated with algal cells. k_1 and k_{-1} are the first-order uptake and depuration rates (in d^{-1}).

$$R_{water} \underset{k_{-1}}{\overset{k_1}{\leftrightarrow}} R_{algae}$$

These rate constants depend on physical-chemical factors such as pH, binding ligands present in the dissolved phase, temperature, etc. The differential equations derived from the kinetic model are

$$\frac{d[R_{water}]}{dt} = -k_1[R_{water}] + k_{-1} \times m_{algae} \times \{R_{algae}\} \quad (1a)$$

$$\frac{d\{R_{algae}\}}{dt} = \frac{k_1}{m_{algae}}[R_{water}] - k_{-1} \times \{R_{algae}\} \quad (1b)$$

where the differential equation systems are expressed on the basis of radionuclide concentration in Bq ml^{-1} ([ ]) or in Bq g^{-1} ww ({ }), with m_{algae}, the algae biomass (in g ml^{-1}, ww).

The uptake and depuration rate constant values, k_1 and k_{-1}, were estimated using the software ModelMaker 3.0.4 (Cherwell Scientific), with the fourth-order Runge-Kutta integration method. Kinetic rate values obtained after two convergence steps are given with the standard error.

The theoretical concentration factor (CF) can be calculated from Eqs. 1a and 1b given the appropriate boundary conditions, under the assumption that, for $t = 0$, all radionuclide was present in the dissolved form ($R_{water(t=0)} = R_{total}$ and $R_{algae(t=0)} = 0$). The solutions for $R_{water}(t)$ and $R_{algae}(t)$ can be used to calculate CF(t) at given times and CF at steady state, with CF expressed in ml g^{-1} ww:

$$CF(t) = \frac{[R_{algae}]}{[R_{water}] \times m_{algae}} = \frac{1}{m_{algae}} \times \frac{1 - e^{-(k_1+k_{-1})\times t}}{\frac{k_{-1}}{k_1} + e^{-(k_1+k_{-1})\times t}} \quad (2)$$

$$CF_{(steady\text{-}state)} = \frac{1}{m_{algae}} \times \frac{k_1}{k_{-1}} \quad (3)$$

For contamination experiments that used natural suspended matter, a similar model was used. The batch was conceptualized as a closed system in which the radionuclide can be adsorbed onto three different components: chlorophytes, bacillariophytes (including diatoms), and other particles (cyanophytes, nonliving mineral, or organic particles). The sorption processes are assumed to work simultaneously and can be modeled by a parallel reaction model that describes the partitioning of radionuclides between the dissolved phase (R_{water}) and the different particulate phases ($R_{Chlorophytes}$, $R_{Bacillariophytes}$, and $R_{Other\ particles}$):

$$R_{water} = \begin{cases} \underset{k_{-1'}}{\overset{k_{1'}}{\rightleftarrows}} R_{Chlorophytes} \\ \underset{k_{-2'}}{\overset{k_{2'}}{\rightleftarrows}} R_{Bacillariophytes} \\ \underset{k_{-3'}}{\overset{k_{3'}}{\rightleftarrows}} R_{Other\ particles} \end{cases}$$

The kinetic rates corresponding to the uptake of radionuclides by the two compartments, ''Chlorophytes'' and ''Bacillariophytes,'' are the values obtained during the first set of experiments with *S. obliquus* and *C. meneghiana* cultures, respectively. The parallel model was used to evaluate the importance of the third compartment, ''Other particles,'' in the kinetic processes characterizing the sorption of radionuclides. The goodness of fit (r^2) and the confidence interval in the estimation of the model parameters were calculated with ModelMaker.

The classical distribution coefficient K_d (in ml g^{-1} ww) was calculated from several runs of the model corresponding to each radionuclide, with an initial waterborne concentration of 1 Bq ml^{-1} and a suspended solid load of 3×10^{-4} g ml^{-1}. The steady-state K_d value was then calculated according to the following equation related to the modeled radionuclide concentrations

$$K_d = \frac{[R_{suspended\ solids}]}{[R_{water}] \times m_{suspended\ solids}} \quad (4)$$

Results and discussion

Radionuclide uptake and depuration patterns for S. obliquus *and* C. meneghiana—The morphology and the growth rates were monitored during experiments. Given the low nutrient content of the Vienne water used during experiments, no significant growth was observed in the case of *C. meneghiana.* The cell volume and surface area were measured as 688 μm^3 and 446 μm^2, respectively. The ratio between the weight and the number of cells was estimated at 1.5×10^{-9} and 1.7×10^{-10} (g $cell^{-1}$), respectively, for the ww and dry weight (dw). In the case of *S. obliquus,* a growth rate of 0.23 d^{-1} was statistically significant for the ^{54}Mn and ^{60}Co uptake experiments. The cells had a weight of 1.1×10^{-10} (g ww $cell^{-1}$) and 2.3×10^{-11} (g dw $cell^{-1}$), a volume of 70 μm^3, and a surface area of 77 μm^2.

The partitioning of radionuclides between dissolved (Vienne water) and solid (phytoplanktonic cells) phases, expressed as a percentage of the initial total activity, was similar for the two algal species, with a rapid increase in par-

Table 1. Fraction of radionuclide associated with the particulate phase during experiments with *S. obliquus* (% of the initial activity for each radionuclide).

Time (h)	^{60}Co	^{137}Cs	^{54}Mn	^{110m}Ag
0	0	0	0	0
0.07	19	5	30	33
0.2	9	4	25	61
0.3	15	6	ND	ND
0.5	27	1	36	48
1	27	5	34	24
2	23	6	42	43
4	25	6	48	47
5.8	30	15	47	48
24	37	9	65	41
31	33	16	67	42
48	43	16	74	45
72	42	31	76	64

ND: Not determined.

Table 2. Fraction of radionuclide associated with the particulate phase during experiments with *C. meneghiana* (% of the initial activity for each radionuclide).

Time (h)	^{60}Co	^{137}Cs	^{54}Mn	^{110m}Ag
0	0	0	0	0
0.07	3	1	26	52
0.2	12	2	ND	ND
0.3	24	1	28	66
0.5	34	4	36	76
1	48	0.3	52	66
2	53	2	85	69
4	56	7	96	77
7	69	8	98	63
24	69	12	82	68
31	69	14	96	53
48	49	15	74	53
72	81	17	89	62

ND: Not determined.

ticulate-phase contamination during the first hour (Tables 1, 2). The greatest affinity for the particulate phase was observed in the case of ^{54}Mn, and the lowest was seen in the case of ^{137}Cs. In the case of *C. meneghiana*, 98% of ^{54}Mn was associated with the particulate phase after 7 h, compared with only 8% for ^{137}Cs.

Radionuclide concentration in the two algae species was plotted against time (Fig. 1). According to the kinetic pat-

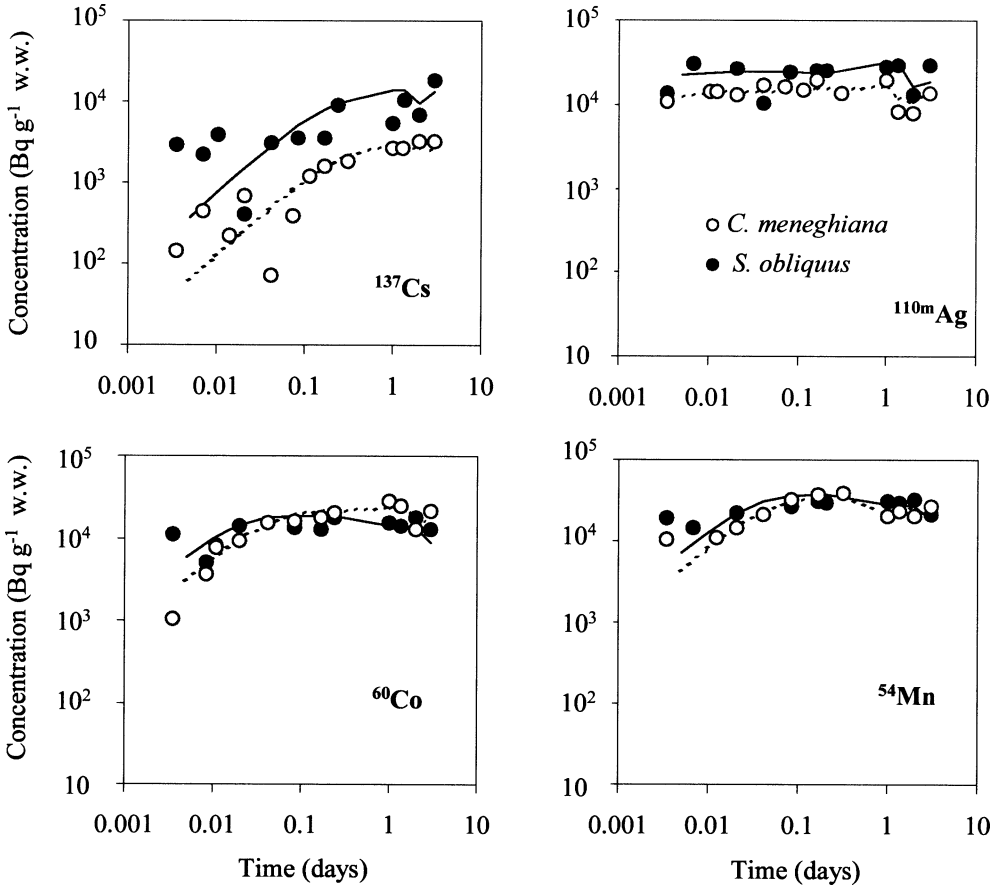

Fig. 1. Uptake of radionuclides (mean ± measurement uncertainty) versus time for *C. meneghiana* and *S. obliquus*. Lines represent the radionuclide concentration, modeled using the one-step reversible kinetic model (solid lines for *S. obliquus* and dotted lines for *C. meneghiana*).

Table 3. Kinetic rates ± standard error (d^{-1}), determined for the transfer of radionuclides to algae using the one-step kinetic model.

Species	^{54}Mn	^{110m}Ag	^{60}Co	^{137}Cs
S. obliquus				
k_1	24.7±7.3	234±84.6	30.1±7.5	1.2±0.43
k_{-1}	17.2±6.2	268±106	58.7±16.6	4.8±1.9
r^2	0.64	0.63	0.64	0.53
C. meneghiana				
k_1	23.7±3.0	293±88.5	20.3±3.6	0.58±0.2
k_{-1}	2.95±0.95	144±47.5	10.5±2.5	3.7±1.5
r^2	0.93	0.79	0.87	0.61

terns and contamination levels, the radionuclides may be separated into three groups. In the case of ^{137}Cs, uptake by the two species was slow, because concentrations reached equilibrium by the second day of exposure. During the first 4 h, a significant scattering of the concentrations was noted, which remained in the case of *S. obliquus* throughout the 3 d. The contamination levels were lower for *C. meneghiana* than for *S. obliquus*, with a maximum concentration of 3,300 versus 18,000 Bq g^{-1} at 3 d of exposure. For ^{110m}Ag, the uptake occurred rapidly, with the first measured values being 11,000 and 13,000 Bq g^{-1}, respectively, for *C. meneghiana* and *S. obliquus*. The plateau was reached within the first hour of the radionuclide spike and from that time on, values remained in the range of 15,000 and 20,000 Bq g^{-1}, respectively, for *C. meneghiana* and *S. obliquus*. ^{60}Co and ^{54}Mn can be classified together in the third group, which was characterized by closer kinetic rates and levels of contamination. Cobalt and manganese concentrations increased until ~6–8 h of exposure, when they stabilized at values of 20,000 (^{60}Co in *S. obliquus*) to 40,000 Bq g^{-1} (^{54}Mn in *C. meneghiana*). From that time on and until the end of the uptake experiment, concentrations exhibited an overall decrease.

The kinetic parameters describing radionuclide transfer were determined using the kinetic model (Table 3). For ^{137}Cs, k_1 values were of the order of 1 d^{-1} for the two algal species. In the case of ^{54}Mn and ^{60}Co, the uptake rates ranged 20–30 d^{-1}, whereas, for ^{110m}Ag, they were higher by an order of magnitude. The depuration kinetic rates (k_{-1}) determined for ^{137}Cs, ^{54}Mn, and ^{60}Co ranged 5–60 and 3–10 d^{-1}, respectively, for *C. meneghiana* and *S. obliquus*. For ^{110m}Ag, k_{-1} values were much higher and reached 270 d^{-1} in the case of *S. obliquus*.

The corresponding $CF_{(steady\text{-}state)}$ (ml g^{-1} ww) values are summarized in Table 4 for each radionuclide and each algae. The highest values were observed for ^{54}Mn (2,770 ml g^{-1} and 9,730 ml g^{-1} for *S. obliquus* and *C. meneghiana*, respectively), and the lowest values were observed for ^{137}Cs (480 ml g^{-1} and 115 ml g^{-1} for *S. obliquus* and *C. meneghiana*, respectively). The surface-normalized CF (in L m^{-2}) and the volume/volume CF (μm^3 μm^{-3}) are also summarized in the table.

Our results can be compared with those of other similar experiments, but the comparison must be considered with caution, because several factors may induce variations in the responses: different algal species (freshwater, euryhaline, or marine), different media (natural freshwater, artificial freshwater, or enriched water), different methodologies (long or short term), and a different characterization of algal uptake (total element or intracellular fraction).

Table 4. Steady-state concentration factors estimated for the radionuclide transfer to *S. obliquus* and *C. meneghiana*.

Species	^{54}Mn	^{110m}Ag	^{60}Co	^{137}Cs
S. obliquus				
Concentration factor (ml g^{-1} ww)	2,770	1,690	990	480
Surface-normalized concentration factor (L m^{-2})	3.8	2.3	1.4	0.7
Volume/volume concentration factor (μm^3 μm^{-3})	4,171	2,536	1,489	726
C. meneghiana				
Concentration factor (ml g^{-1} ww)	9,730	1,450	2,240	115
Surface-normalized concentration factor (L m^{-2})	32.4	4.8	7.5	0.4
Volume/volume concentration factor (μm^3 μm^{-3})	20,992	3,118	4,840	245

A wide range of CF values for silver has been found by other authors. Garnier and Baudin (1989) found a CF of 4×10^5 (ml g^{-1} ww) for ^{110m}AgCN uptake by *S. obliquus*. Terhaar et al. (1977) determined a CF of 6,000 ml g^{-1} ww for silver thiosulfate bioaccumulation by the same species, contaminated under semicontinuous conditions. Fortin and Campbell (1999) calculated a surface-normalized CF value of 120 L m^{-2} for intracellular silver uptake by the green alga *Chlamydomonas reinhardtii*. For diatoms, no data could be found for freshwater species. Reinfelder and Chang (1999) determined, for the large marine diatom *Thalassiosera weissflogii* (cell volume of 10^3 μm^3), a CF ranging 2,500–3,200 μm^3 μm^{-3} for different *p*Cl (3.3–1.3). Our CF value of 3,200 μm^3 μm^{-3} determined for *C. meneghiana* and for a *p*Cl of 3.3 is in agreement with these values.

For cobalt, Nucho et al. (1988) determined different CF values, ranging 310–3,300 ml g^{-1} ww for *S. obliquus* cultures aged 6–21 d. Similar experiments were also conducted in two natural-medium hard waters (Nucho 1989) in which a CF of 2,000 ml g^{-1} ww was observed. Our CF value of 990 ml g^{-1} ww falls within the range of CF values calculated by those authors. In the case of diatoms, *C. meneghiana* was contaminated by ^{60}Co in 0.22-μm filtered water of the Meuse River (Belgium) that had been enriched with nitrates, phosphates, and silica (Anonymous 1987). The CF observed after a contact time of 48 h was of the order of 600 ml g^{-1} ww. Fortin and Campbell (2000) studied Mn accumulation by *C. reinhardtii* in a low (5 μmol L^{-1}) or high (4 mmol L^{-1}) chloride medium at an ionic strength of 6 meq L^{-1}. CFs calculated from their results ranged 0.6–0.75 L m^{-2} at 1 h, which is of the same order of magnitude as our value of 2.5 L m^{-2}.

In the case of Cs, Sombré et al. (1993) found a CF of 20 ml g^{-1} ww for the transfer of ^{134}Cs to *S. obliquus* in a tur-

bidostat culture and for an artificial culture medium. Gil Corrisco and Vaz Carreiro (1990) determined a CF of 354 ml g^{-1} ww for ^{134}Cs transfer to *Selenastrum capricornutum,* which is close to the steady-state CF calculated in the present study (480 ml g^{-1} ww).

Various mechanisms may be involved in trace element uptake by microalgae. The cell wall is able to bind metal cations with its negatively charged sites, polysaccharides, and some unprotonated groups such as carboxyl oxygen and sulphate (Campbell and Stockes 1985). Nieboer and Richardson (1980) proposed a classification of metal ions based on the biological and chemical availability to organisms as a function of their binding preferences. This classification takes into account atomic number, specific gravity, ionic radius, thermodynamic equilibrium constants, and metal-ion electronegativity. According to this classification scheme, cesium belongs to class A (oxygen-seeking), silver to class B (sulphur-seeking), and cobalt and manganese to borderline class (intermediate properties), which confirms our own classification of the radionuclides.

As demonstrated by Fortin and Campbell (2000), silver uptake is by definition accidental, because it is not a micronutrient. They showed that silver was probably transported through a Cu(I) system, which can explain the very high uptake and depuration rates observed for our ^{110m}Ag experiments.

Cobalt is a component of vitamin B_{12}; as a consequence, it is essential for most living organisms. It can also be incorporated into superoxide dismutases, which play an important role in the defense mechanisms against oxidative stress (Meier et al. 1994). The mechanism of cobalt uptake was investigated by Liu et al. (1998) using cells of the giant freshwater alga *Chara corallina.* The transported chemical species appears to be Co^{2+}, which is probably transported by thiol groups in membrane transporters. That influx is inhibited by Cd^{2+}, Cu^{2+}, and Zn^{2+}, but Mn^{2+} and Ni^{2+} have no significant effect, which suggests that Mn^{2+} is not internalized by the same transporter. They showed that the adsorption of cobalt into the cell wall accounted for 90% of the total activity, the prevailing mechanism being ionic exchange. It appears that part of the cobalt that is trapped in the cell wall is not bioavailable: Macfie et al. (1994) demonstrated the protective role of the cell wall against cobalt toxicity by comparing EC_{30} in walled and wall-less strains of *C. reinhardtii.*

Like cobalt, manganese is an essential nutrient, and numerous enzymes use the redox properties of this element. It is essential for catalyzing oxygen development in photosynthesis (Raven et al. 1999), and mitochondrial Mn superoxide dismutase has been identified as a major scavenger of O_2^- produced during photosynthesis (Okamoto and Colepicolo 2001). The main mechanism of Mn accumulation seems to be the formation of Mn oxides on algal surfaces. Stuez et al. (1996) found high amounts of Mn(III) and Mn(IV) oxides on the surface of *Chlamydomonas* cells. The same result was found by Knauer et al. (1999) for *Scenedesmus subspicatus.* Those authors showed that <5% of the total cellular manganese was bound as Mn^{2+} to negatively charged polymers, whereas >90% of the total manganese occurred in the form of Mn(III) and Mn(IV) oxides. Moreover, they showed that small manganese oxides were associated with the algae. However, this was questioned by Abu-Shammala (1999), who did not observe any Mn on the surface of *Chlamydomonas* or *Chlorella* using X-ray microanalysis. Mn is then internalized by a saturable uptake system that is under negative feedback control by some intracellular pool, as was shown for *C. reinhardtii* by Sunda and Huntman (1998). In *Chlamydomonas, Chlorella,* and *Anabeana,* Mn was localized by X-ray analysis in intracellular bodies that were presumed to be polyphosphate inclusions (Abu-Shammala 1999).

In the case of Cs, uptake mechanisms have been very rarely studied for phytoplankton species. Pagis et al. (2001) showed that Cs was transported inside the halotolerant alga *Tetraselmis viridis* through the potassium channel but not by the Na^+/H^+ antiporter or Na^+-ATPase, which seem to be specific to Na^+ and Li^+.

The surface-normalized CF (SCF) summarized in Table 4 for *S. obliquus* and *C. meneghiana* provides a means to compare the uptake specificities for each alga. For *S. obliquus,* the SCF values are not very different for the four radionuclides, ranging 0.7–3.8 L m^{-2}, whereas, for *C. meneghiana,* there are almost 2 orders of magnitude separating manganese and cesium SCFs. The SCFs calculated for *C. meneghiana* are higher than those determined for *S. obliquus,* the greatest difference being observed for Mn (8.5-fold), then Co (5.4-fold) and Ag (2.1-fold). In the case of cesium, the SCF value is lower for *C. meneghiana* than that for *S. obliquus,* but the very narrow range of SCFs obtained for this radionuclide suggests that the difference may not be significant. The high SCF observed for manganese uptake by *C. meneghiana* could indicate that Mn oxidation occurred at the cell surface. It is well known that photosynthesizing algae can generate microenvironments with pH values >9. Richardson and Stolzenbach (1995) showed that Mn oxidation depends on the cell size of algae, which indicates that cells larger than 20 μm can induce Mn oxidation. Even for *S. subspicatus,* which consists of small cells not likely to build up a large pH gradient at their surface, Knauer et al. (1999) showed that a large fraction of Mn bound by this alga occurred as Mn(III/IV) oxides. This microenvironmental change of physical-chemical conditions surrounding the algae may be more drastic for *C. meneghiana* that is characterized by a cell surface area of 446 μm^2, leading to a higher Mn oxidation rate at the surface of the diatom than *S. obliquus,* which has a smaller surface area of 77 μm^{-2}.

Other hypotheses linked to comparisons of the characteristics of the cell walls and the membranes of green algae and diatoms could explain the differences in SCF observed. Kiefer et al. (1997) used different chemical and spectroscopic methods to characterize the surfaces of *Cyclotella cryptica* and *C. reinhardtii.* The surface groups were analyzed using Fourier-transform infrared spectroscopy (FT-IR) and acid-base titration curves. The green algae surface contained a larger variety of weaker acid-base groups than the surface of the diatom. The FT-IR spectrum of *C. cryptica* showed only two kinds of functional groups (NH_2 and Si-OH), whereas that of *C. reinhardtii* showed a wide variety of functional groups (R-COOH, R-OH, CN^-, and NH_2, etc.). These binding sites can be related to the chemical and bio-

Table 5. Main characteristics of the Vienne water collected for the contamination experiment of natural suspended solids.

Dissolved organic carbon (mg L^{-1})	6.5
Total organic carbon (mg L^{-1})	7
Chlorophyll *a* (mg m^{-3})	20
Suspended solids (mg L^{-1})	25.7
Organic suspended solids (mg L^{-1})	4
Temperature (°C)	24.5
Median diameter (μm)	35.1
pH	7.2
Conductivity (μS cm^{-1})	188
Ca^{2+} (mg L^{-1})	17
Mg^{2+} (mg L^{-1})	2
Cl^- (mg L^{-1})	18
HCO_3^- (mg L^{-1})	63

logical properties of the four radionuclides, according to the classification of Nieboer and Richardson (1980). Mn^{2+} and Co^{2+} are borderline ions with considerable class A character, which indicates that they will bind strongly to nitrogen- and oxygen-containing functional groups. Ag^+ is a class B ion that binds preferentially to sulphur centers and then to nitrogen functional groups. Cs^+ belongs to class A and binds to oxygen centers. These binding preferences may explain why the ^{137}Cs accumulation level was higher for the green algae *S. obliquus,* which probably has the same surface functional groups as *C. reinhardtii* (mainly O-donor type) and why ^{54}Mn, ^{60}Co, and ^{110m}Ag were accumulated to a higher extent by *C. meneghiana,* which is characterized by nitrogen functional groups. Another hypothesis could be that diatoms act as a cation's trap because they are constituted of a silica frustule encased in an organic coating (Rince et al. 1999; Wang et al. 2000). Finally, different internalization mechanisms are probably induced in the two species (Rijstenbil et al. 1994), which could also explain the observed differences.

Radionuclide uptake and depuration patterns for natural suspended matter—The main characteristics of the water (dissolved and particulate phase) collected in July for natural suspended matter contamination are summarized in Table 5. The results are consistent with other data collected on the same river (Garnier et al. 1997). Chl *a* content (20 mg m^{-3}) and pH value are indicative of a bloom event. If these values are low compared with bloom events observed in other rivers such as the Loire (Lair and Reyes-Marchant 1997; Lair et al. 1999), it is because the Vienne River has turbid and highly colored water, which limits phytoplankton development. Despite these physical-chemical characteristics, the algal flora is rich and abundant. More than 30 genera have been identified, and the total number of cells is 3.2×10^4 cells ml^{-1}. The green algae were dominant, representing 65% of the total cells number. The chlorococcales *Scenedesmus* were the most abundant (5×10^3 cells ml^{-1}) and were associated with other chlorophytes such as *Staurastrum* (2.8×10^3 cells ml^{-1}), *Actinastrum* (2.6×10^3 cells L^{-1}), and *Closterium* (2.4×10^3 cells ml^{-1}). Among the bacillariophytes, which represented 19% of the algal genera identified, the small centric diatom *Cyclotella* was the most abundant (2.6×10^3 cells ml^{-1}), associated with *Synedra, Navicula,* and *Stephanodiscus.* The cyanobacteria population was dominated by *Oscillatoria* (3.2×10^3 cells ml^{-1}) and *Chroococcus* (1.5×10^3 cells ml^{-1}). The phytoplankton collected was mainly composed of holoplankton, which multiplies in the water column. Associations of *Cyclotella-Stephanodiscus* or *Cyclotella-Scenedesmus,* which are characteristic of eutrophic waters, have been reported in other temperate rivers such as the Thames (Lack 1971) and the Loire (Lair et al. 1999). The relative composition of phytoplanktonic population changed from the third day, probably because of nitrogen depletion in the medium, which favors cyanophycae growth. That class represented >50% of the phytoplankton population from the third day. In parallel, although the water was not supplemented with nutrients, to limit changes in radionuclide speciation, populations of green algae and bacillariophytes were doubled within 3 d.

Table 6. Fraction of radionuclide associated with the particulate phase during experiments with natural suspended matter (% of the initial activity for each radionuclide).

Time (h)	^{60}Co	^{137}Cs	^{54}Mn	^{110m}Ag
0.000	0	0	0	0
0.07	19	ND	53	34
0.17	38	3	76	46
0.24	47	4	ND	48
0.5	64	4	90	47
0.7	57	5	92	51
1	72	6	93	57
2	87	8	97	58
3	93	13	97	56
4	94	9	97	57
8	97	15	98	65
26	98	15	98	67
32	98	12	98	64
44	97	21	98	58
68	97	17	98	62

ND: Not determined.

The fraction of radionuclide present in the particulate phase was monitored throughout the 3-d uptake experiment (Table 6). For ^{137}Cs, the percentage of radionuclide sorbed against time was similar to the values observed for *S. obliquus* and *C. meneghiana,* and the process was slow and weak, given that only 9% was associated with particles after 4 h. After the first day, the contamination of suspended solids by this radionuclide remained stable at $\sim 1.5 \times 10^4$ Bq g^{-1}. In the case of ^{110m}Ag, more than half of the total amount was sorbed onto particles within the first exposure hour, which was in the range of the values observed for *S. obliquus* and *C. meneghiana.* The concentrations measured in the suspended solids from the onset of the plateau phase were of the order of 4.5×10^4 Bq g^{-1}. In the case of ^{54}Mn and ^{60}Co, the sorption phenomenon was faster for natural suspended solids than for *S. obliquus* and *C. meneghiana.* In the case of cobalt, the percentage retained by particles increased from two- to fourfold, depending on the sampling time. For ^{54}Mn, the amount found in the particulate phase was 90% at 30 min, and this value reached 98% after 4 h of exposure. The particulate concentrations of ^{60}Co and ^{54}Mn were much greater than those observed for ^{137}Cs and ^{110m}Ag,

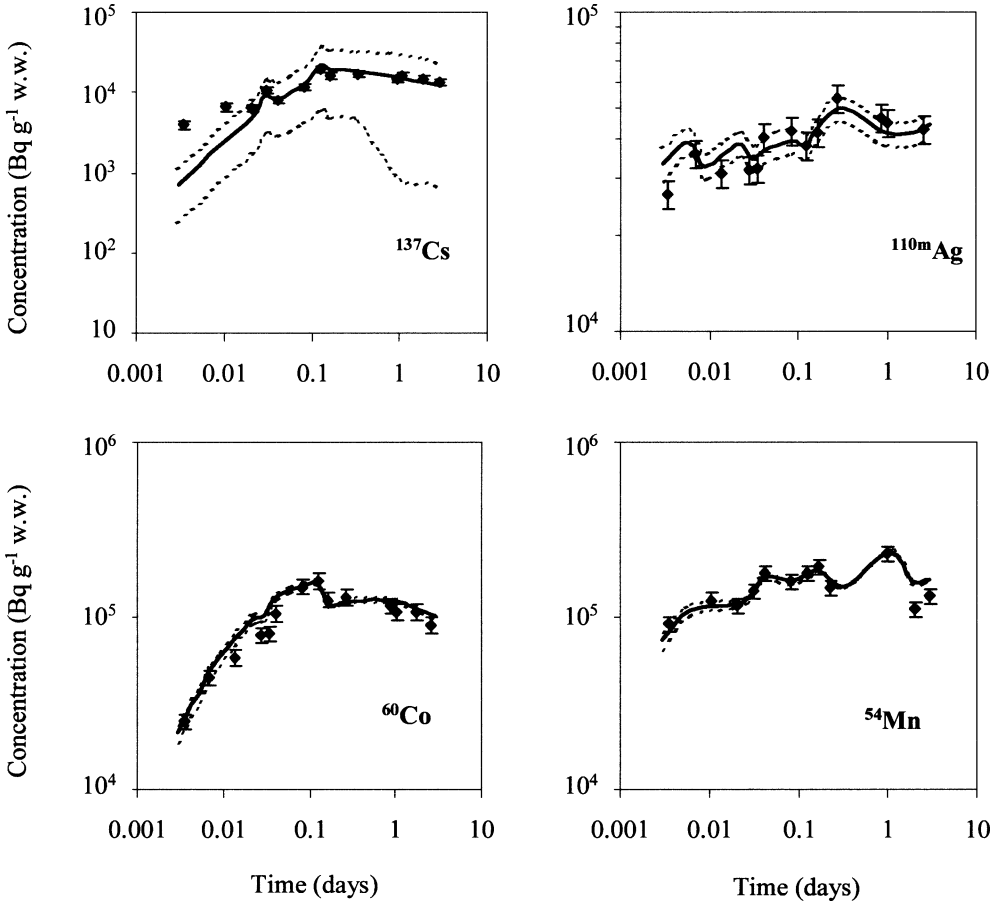

Fig. 2. Uptake of radionuclides (mean ± measurement uncertainty) versus time by natural suspended solids collected during a summer bloom period. Solid lines represent the radionuclide concentration, modeled using the parallel reaction kinetic model. Dashed lines represent the confidence interval of the model, calculated using the standard deviation on the kinetic parameters.

with equilibrium values of $\sim 1.2 \times 10^5$ and 2.4×10^5 Bq g^{-1} for cobalt and manganese, respectively.

The parallel reaction model was used to evaluate the validity field of the kinetic rates estimated for *S. obliquus* and *C. meneghiana* applied to a summer bloom (Fig. 2). The modeled concentrations are shown, along with the confidence interval calculated with ModelMaker according to the standard error associated with the kinetic parameters used. The kinetic rates estimated are summarized in Table 7. According to the number of identified processes, the four radionuclides can again be separated into three groups. In the particular case of ^{137}Cs, vessel wall was added as a fourth compartment, to take into account the high adsorption evidenced. Despite this correction, the observed data could not be fitted with a parallel reaction model using the kinetic rates estimated for *S. obliquus* and *C. meneghiana.* As a consequence, a simple model was used with one compartment representing the suspended solids and a second one the tank walls. The uptake and depuration rate values corresponding to the suspended solid compartment were estimated, respectively, at 1.6 ± 1.1 and 9.5 ± 8 d^{-1}. For ^{110m}Ag, the two compartments representing the green algae and the diatoms were sufficient to describe the natural suspended solids contamination. For ^{54}Mn and ^{60}Co, the experimental data could be fitted by a three-compartment model. Two compartments corresponded to the green algae and the diatoms, their contamination being described by the kinetic rates estimated from the first set of laboratory experiments. A third compartment could be identified, with corresponding uptake and depuration rates of 17 ± 3 and 1.2 ± 0.8 d^{-1} for ^{60}Co and 220 ± 50 and 27 ± 16 d^{-1} for ^{54}Mn.

These modeled data are shown in Fig. 3 as the fraction of

Table 7. Kinetic rates ± standard error (d^{-1}), determined for the transfer of radionuclides to suspended solids using the parallel-reaction model.

Kinetic rate	^{54}Mn	^{110m}Ag	^{60}Co	^{137}Cs
k'_3	216±47	—*	16.6±3.4	1.62±1.06†
k'_3	27.4±16	—*	1.2±0.8	9.5±7.6†
r^2	0.90	0.91	0.90	0.75

* Experimental data fitted with chlorophyte and bacillariophyte compartment only.

† Estimated with a different conceptual model than to the other radionuclides.

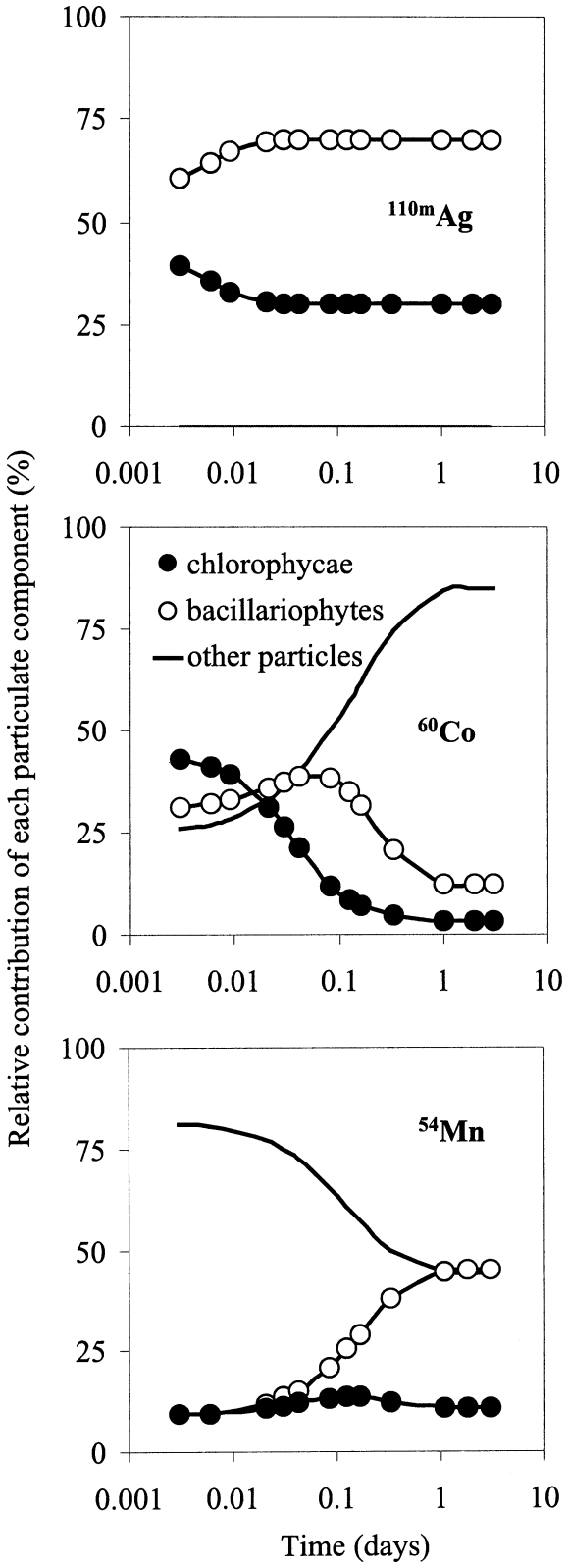

Fig. 3. Theoretical relative contribution of each particulate component to the total amount of radionuclide sorbed, modeled using the parallel reaction kinetic model. Kinetic rates corresponding to chlorophycae and bacillariophytes uptake were set to the values obtained under laboratory conditions for *S. obliquus* and *C. meneghiana.* Kinetic rates corresponding to the contamination of other particles (minerals, blue-green algae, etc.) were optimized using ModelMaker. A single compartment was fitted in the case of cesium.

radionuclide adsorbed onto each compartment, which represents the importance of the distinct processes (^{137}Cs is not shown, because only one process could be identified). In the case of ^{110m}Ag, the two compartments corresponding to radionuclide uptake by green algae and diatom communities are represented. The amount of silver accumulated by the diatom community represents ~70% of the total radionuclide measured in the particulate phase. The equilibrium between the two algal compartments was achieved within the first hour. As regards ^{60}Co, no equilibrium was observed during the first day, with a variation of relative activity for the three compartments. During the first day, the third compartment rose until its contribution represented 85% of the total particulate element after 24 h. At that time, the diatom community contributed 12% of total radioactivity and green algae 3%. A similar mechanism is observed for ^{54}Mn. The third compartment contribution decreased from 80% to 44% during the first day, whereas, during the same time, the diatom contribution rose from 10% to 44%. The green algae community contribution did not vary significantly during the 3 d, and the accumulated amount represented ~12% of the total radioactivity in the particulate phase. On this basis, steady-state K_d values ranged 570 ml g^{-1} ww for ^{137}Cs, 9.7 $\times$ 10^3 for ^{110m}Ag, 5.3 $\times$ 10^4 for ^{60}Co, and 6.0 $\times$ 10^4 for ^{54}Mn.

Garnier-Laplace et al. (1997) showed, in their review of radionuclide exchanges among water, suspended solids, and sediments, that the K_d values were governed by a variety of factors, depending on the characteristics of the liquid and solid phases. As a consequence, for cesium, cobalt, and manganese, the K_d values obtained from the relevant literature range from 1 to 100 m^3 kg^{-1} dw, and, for silver, the range spanned three orders of magnitude (0.1–100 m^3 kg^{-1} dw). For that reason, it does not make any sense to quantitatively compare our results with those of other water systems, and only the processes involved will be discussed.

It is important to keep in mind that the different kinetic rates fitted with this parallel reaction model do not necessarily represent specific chemical or biological reactions but simply provide a basis for discriminating between the various absorption and desorption processes. In the case of ^{54}Mn, the third compartment is characterized by very fast uptake and by slower desorption. The kinetic values fitted could be attributed to manganese oxidation, but they do not correspond to the long reaction time of Mn oxidation (35 d) calculated by Sung and Morgan (1981), which should be described by much lower kinetic rates. This may be explained by the presence of bacteria and microalgae, that facilitate Mn(II) oxidation, as shown by Stuez et al. (1996). Furthermore, an important adsorption role may be played by cyanophycae, as shown by Abu-Shammala (1999), who found large amounts of manganese in the external mucilaginous layer surrounding *Anabaena* cells.

A third compartment was also fitted for ^{60}Co using lower values for the kinetic constants. The influence of bacteria on cobalt sorption has been shown by Sibley et al. (1981), who

also observed high cobalt sorption on organic dead material. Moreover, cobalt is known to be easily trapped in MnO_2 coating on particles. This fact was confirmed by Garnier et al. (1997), who compared the kinetics of trace element complexation with suspended solids also collected in the Vienne River during a summer bloom event and during winter. They showed that Mn and Co $K_d(t)$ were correlated, which confirms the high affinity of manganese oxides for cobalt. Moreover, they concluded that Mn and Co removal was controlled by binding with particulate organic matter and biogenic particles. These different processes of cobalt complexation probably occur simultaneously and are integrated into the third compartment in the model fits.

In the case of silver, no kinetic constant could be fitted for the third compartment. This does not necessarily mean that silver adsorption by other components does not occur but that it is governed by similar kinetic patterns as those estimated for *S. obliquus* and *C. meneghiana.* However, a preeminence of silver uptake by algae is not surprising, given the extremely high bioavailability of silver demonstrated by Fortin and Campbell (2000).

Finally, as concerns ^{137}Cs, the kinetic parameters fitted for *S. obliquus* and *C. meneghiana* could not be used to model suspended solid contamination. A single compartment was described by very slow uptake and faster desorption. Nyffeler et al. (1984) studied radionuclide distribution between seawater and particles, according to a similar kinetic model. They also found low values for ^{134}Cs kinetic parameters—the uptake kinetic parameter was determined as 0.0236 d^{-1} and the desorption constant as 1.0 d^{-1}, with a very low corresponding K_d value ($\sim$100 L kg^{-1}). This is consistent with the well-known low affinity of cesium for particulate organic matter and its high affinity for clay minerals (Garnier-Laplace et al. 1997). Moreover, it can be hypothesized that organic coating onto particles does not facilitate Cs adsorption.

The results presented here show that the processes governing suspended matter during a bloom event are very different for Ag, Co, Cs, and Mn. Biological processes dominate silver uptake, and the kinetic rates determined for unialgal species during laboratory experiments can be used. For Mn and Co, additional chemical and/or biological processes due, for instance, to cyanophycae contamination have to be taken into account. Finally, the low bioavailability of Cs was confirmed, and its partitioning should rather be described by electrostatic interaction between Cs^+ and negatively charged particle surfaces or by cation exchange of Cs^+ with K^+ channels or the interlayer position of clay minerals.

References

ABU-SHAMMALA, F. 1999. Localisation of manganese accumulated by microalgal cells using energy-dispersive X-ray microanalysis in the electron microscope. Asian J. Chem. **11:** 819–835.

ANONYMOUS. 1987. Etude comparée de la radioécologie des eaux continentales des bassins Mosab et Rhodanien. Contribution des Laboratoires Belges. European Community report CEE B16-B-040-B.

CAMPBELL, P. C. G., AND P. M. STOCKES. 1985. Acidification and toxicity of metals to aquatic biota. Can. J. Fish. Aquat. Sci. **42:** 2034–2049.

FLORENCE, T. M., G. M. MORRISON, AND J. L. STAUBER. 1992. Determination of trace element speciation and the role of speciation in aquatic toxicity. Sci. Tot. Environ. **125:** 1–13.

FORTIN, C., AND P. G. C. CAMPBELL. 1999. Thiosulfate enhances silver uptake by a green alga: Role of anion transporters in metal uptake. Environ. Sci. Technol. **35:** 2214–2218.

———, AND ———. 2000. Silver uptake by the green alga *Chlamydomonas reinhardtii* in relation to chemical speciation: Influence of chloride. Environ. Toxicol. Chem. **19:** 2769–2778.

GARNIER, J., AND J.-P. BAUDIN. 1989. Accumulation and depuration of ^{110m}Ag by a planktonic alga, *Scenedesmus obliquus.* Water Air Soil Pollut. **45:** 287–299.

———, M. K. PHAM, P. CIFFROY, AND J.-M. MARTIN. 1997. Kinetics of trace element complexation with suspended matter and with filterable ligands in freshwater. Environ. Sci. Technol. **31:** 1597–1606.

GARNIER-LAPLACE, J., V. FOURNIER-BIDOZ, AND J.-P. BAUDIN. 1997. Etat des connaissances sur les échanges entre l'eau, les matières en suspension et les sédiments des principaux radionucléides rejetés en eau douce par les centrales nucléaires. Radioprotection **32:** 49–71.

GIL CORRISCO, J. A., AND M. C. VAZ CARREIRO. 1990. Etude expérimentale sur l'accumulation et la rétention du ^{134}Cs par une microalgue planctonique, *Selenastrum capricornutum* Printz. Rev. Sci. Eau **3:** 457–468.

GUILLARD, R., AND J. RYTHER. 1962. Studies of marine planktonic diatoms. 1. *Cyclotella nana* hustedt and *Detonula confervacea* (cleve) gran. Can. J. Microbiol. **8:** 229–239.

JANNASCH, H. W., B. D. HONEYMAN, L. S. BALISTRIERI, AND J. W. MURRAY. 1988. Kinetics of trace elements uptake by marine particles. Geochim. Cosmochim. Acta **52:** 567–577.

KIEFER, E., L. SIGG, AND P. SCHOSSELER. 1997. Chemical and spectroscopic characterization of algae surfaces. Environ. Sci. Technol. **31:** 759–764.

KNAUER, K., T. JABUSCH, AND L. SIGG. 1999. Manganese uptake and Mn(II) oxidation by the alga *Scenedesmus subspicatus.* Aquat. Sci. **61:** 44–58.

KUDO, I., T. OHYAMA, S. NAKABAYASHI, K. KUMA, AND K. MATSUNAGA. 1992. Behavior and dynamic balance of manganese during spring bloom in Funka Bay, Japan. Mar. Chem. **40:** 273–289.

LACK, T. J. 1971. Quantitative studies on the phytoplankton of the river Thames and Kennet: A reading. Freshw. Biol. **1:** 213–224.

LAIR, N., V. JACQUET, AND P. REYES-MARCHANT. 1999. Factors related to autotrophic potamoplankton, heterotrophic protists and micrometazoan abundance, at two sites in a lowland temperate river during low water flow. Hydrobiologia **394:** 13–28.

———, AND P. REYES-MARCHANT. 1997. The potamoplankton of the Middle Loire and the role of the ''moving littoral'' in downstream transfer of algae and rotifers. Hydrobiologia **356:** 33–52.

LIU, J., J. REID, AND F. A. SMITH. 1998. Mechanisms of cobalt uptake in plants: ^{60}Co uptake and distribution in *Chara.* Physiol. Plant **104:** 351–356.

MACFIE, S. M., Y. TARMOHAMED, AND P. M. WELBOURN. 1994. Effects of cadmium, cobalt, copper and nickel on growth of the green alga *Chlamydomonas reinhardtii:* The influences of the cell wall and pH. Arch. Environ. Contam. Toxicol. **27:** 454–458.

MEIER, B., A. P. SEHN, M. SETTE, M. PACI, A. DESIDERI, AND G. ROTILIO. 1994. In vivo incorporation of cobalt into *Propionibacterium shermanii* superoxide dismutase. FEBS Lett. **348:** 283–286.

MOFFETT, J. W. 1994. A radiotracer study of cerium and manganese

uptake onto suspended particles in Cheasapeake Bay. Geochim. Cosmochim. Acta. **58:** 695–703.

NICHOLS, H. W., AND H. C. BOLD. 1965. *Tricosarcina polymorpha et sp. nov.* J. Phycol. **1:** 34–38.

NIEBOER, E., AND D. H. S. RICHARDSON. 1980. The replacement of the nondescript term ''heavy metals'' by a biologically and chemically significant classification of metal ions. Environ. Pollut. B **1:** 3–26.

NUCHO, R. 1989. Modalités de la fixation et de la désorption du ^{60}Co par *Scenedesmus obliquus* et transfert du radioélément vers deux organismes benthiques. Ph.D. thesis, Univ. of Montpellier I.

———, A. RAMBAUD, L. FOULQUIER, AND J.-P. BAUDIN. 1988. Bioaccumulation du ^{60}Co par une algue planctonique *Scenedesmus obliquus.* Influence du stade de développement de la culture sur la fixation du radionucléide. Acta Oecol. Oecol. Appl. **9:** 111–125.

NYFFELER, U. P., Y. H. LI, AND P. SANTSCHI. 1984. A kinetic approach to describe trace-element distribution between particles and solution in natural aquatic systems. Geochim. Cosmochim. Acta **48:** 1513–1522.

OKAMOTO, O. K., AND P. COLEPOCOLO. 2001. Circadian protection against reactive oxygen species involves changes in daily levels of manganese and iron containing superoxide dismutase isoforms in *Lingulodinium polyedrum.* Biol. Rhythm Res. **32:** 439–448.

PAGIS, L. Y., L. G. POPAVA, I. M. ANDREEV, AND Y. V. BALNOKIN. 2001. Ion specificity of Na+ transporting systems in the plasma membrane of the halotolerant alga *Tetraselmis (Platymonas) viridis.* Russ. J. Plant Physiol. **48:** 281–286.

RAVEN, J. A., M. C. W. EVANS, AND R. E. KORB. 1999. The role of trace metals in photosynthetic electron transport in O_2 evolving organisms. Photosynth. Res. **60:** 111–149.

REINFELDER, J. R., AND S. I. CHANG. 1999. Speciation and microalgal bioavailability of inorganic silver. Environ. Sci. Technol. **33:** 1860–1863.

RICHARDSON, L. L., AND K. D. STOLZENBACH. 1995. Phytoplankton cell size and the development of microenvironments. FEMS Microbiol. Ecol. **16:** 185–192.

RIJSTENBIL, J. W., A. SANDEE, J. VANDRIE, AND J. A. WJNHOLDS. 1994. Interaction of toxic trace-metals and mechanisms of detoxification in the planktonic diatoms *Ditylum brightwellii* and *Thalassosiria pseudonana.* FEMS Microbiol. Rev. **14:** 387–396.

RINCE, Y., T. LEBEAU, AND J. M. ROBERT. 1999. Artificial cell immobilization: A model simulating immobilization in natural environments? J. Appl. Phycol. **11:** 263–272.

SCHOEMANN, V., H. J. W. DEBAR, J. T. M. DE JONG, AND C. LANCELOT. 1998. Effects of phytoplankton blooms on the cycling of manganese and iron in coastal waters. Limnol. Oceanogr. **43:** 1427–1441.

SIBLEY, T. H., A. L. SANCHEZ, AND W. R. SCHELL. 1981. Distribution coefficients for radionuclides in aquatic environments: Adsorption studies of cobalt. NUREG/CR-1852, vol. 6. College of Fisheries, Univ. of Washington.

SOMBRÉ, L., Y. THIRY, AND C. MYTTENAERE. 1993. The radiocesium transfer in a freshwater food chain (water-algae-mussels-fish-fish). J. Radioecol. **1:** 21–27.

STUEZ, R. M., A. C. GREENE, AND J. C. MADGWICK. 1996. Microalgal-facilitated bacterial oxidation of manganese. J. Industr. Microbiol. **16:** 267–273.

SUNG, W., AND J. J. MORGAN. 1981. Oxidative removal of Mn(II) from solution catalysed by the gamma-FeOOH (lepidocrite) surface. Geochim. Cosmochim. Acta **45:** 2377–2383.

SUNDA, W. G. 1988. Trace metal interactions with marine phytoplankton. Biol. Oceanogr. **6:** 411–442.

———, AND S. A. HUNTSMAN. 1987. Microbial oxidation of manganese in North Carolina estuary. Limnol. Oceanogr. **32:** 552–564.

———, AND ———. 1998. Interactions among Cu^{2+}, Zn^{2+}, and Mn^{2+} in controlling cellular Mn, Zn, and growth rate of the coastal alga *Chlamydomonas.* Limnol. Oceanogr. **43:** 1055–1064.

TERHAAR, C. J., W. S. EWELL, S. P. DZIUBA, W. W. WHITE, AND P. J. MURPHY. 1977. A laboratory model for evaluating the behaviour of heavy metals in an aquatic environment. Water Res. **11:** 101–110.

WANG, Y., Y. CHEN, C. LAVIN, AND M. R. GRETZ. 2000. Extracellular matrix assembly in diatoms (Bacillariophycae). IV. Ultrastructure of *Achnanthes longipes* and *Cymbella cistula* as revealed by high-pressure freezing/freeze substitution and cryo-field emission scanning electron microscopy. J. Phycol. **36:** 367–378.

Received: 9 September 2002
Amended: 5 May 2003
Accepted: 23 May 2003